

# A Numerical Procedure for Calculating the Integrated Acoustooptic Effect

BILL D. COOK, SENIOR MEMBER, IEEE, EDUARDO CAVANAGH, AND HENRY D. DARDY, MEMBER, IEEE

**Abstract**—The integrated optical effect of light passing through an ultrasonic field can be numerically calculated from the velocity distribution assigned to a planar transducer. The theory is developed for linear acoustics, nonabsorbing media, and normal incidence of light. As a consequence of the application of the Fourier projection slice theorem, an algorithm based on digital Fourier transforms calculates the integrated optical effect without integration. Demonstrations of the influence of transducer geometry are shown for the integrated optical effect and schlieren patterns based on this effect.

## INTRODUCTION

THE OPTICAL methods for estimating field quantities, such as pressure, of ultrasonic fields required a model of the sound field. Often these were simplistic (collimated plane waves) but very useful. In reality the light usually passes through the near-field region of the ultrasonic transducer. The multitude of schlieren photographs in the literature give testimony to the complexity of the effect of the near field. For example, Fig. 1 shows a schlieren image, published by Osterhammel [1] in 1941, of the near field of a square transducer. The intricate pattern was explained by Osterhammel as interference of plane waves from the face of transducer and circular waves from the edge; this theory does not permit quantitative calculations and is not extendable to other geometries.

Schlieren patterns such as is shown in Fig. 1 can be computed provided the field parameters of the integrated optical effect are known. At low ultrasonic frequencies, the interaction of sound and light can be described by one parameter, the so-called Raman-Nath parameter  $\nu$  [2]. For a three-dimensional pressure field  $p(x, y, z) e^{i\omega t}$ , with the light traversing in the  $y$  direction as shown in Fig. 2, the integrated optical effect is defined as

$$\nu(x, z) = \frac{2\pi\kappa}{\lambda} \int p(x, y, z) dy. \quad (1)$$

Here  $\lambda$  is the optical wavelength and  $\kappa$  is the piezooptic coefficient. The integrated optical effect is thus a two-dimensional phasor field  $\nu(x, z)$ . In this paper a computation procedure is presented for calculating  $\nu(x, z)$  when the motion of the transducer is specified. The procedure is straightforward and eased

Manuscript received December 5, 1979; revised March 1, 1980. This work was supported in part by the Office of Naval Research in conjunction with the Physical Acoustics Branch, Navy Research Laboratory, Washington, DC.

B. D. Cook and E. Cavanagh are with the Cullen College of Engineering, University of Houston, Central Campus, Houston, TX 77004.

H. D. Dardy is with the Naval Research Laboratory, Washington, DC 20375.

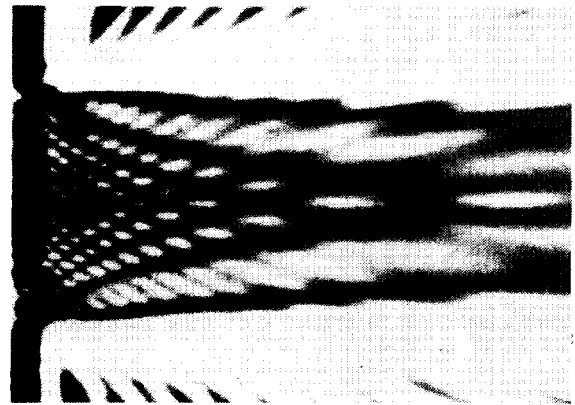


Fig. 1. Schlieren photograph of near field of a square transducer with ratio of width to acoustical wavelength of 14.37, from Osterhammel [1].

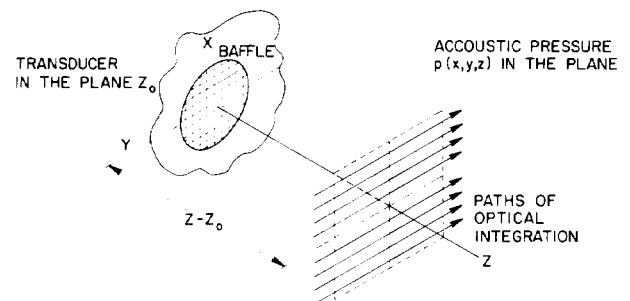


Fig. 2. Diagram showing geometry.

by utilization of the standard one-dimensional Fourier transform which yields the field  $\nu(x, z)$  at a given  $z$  as a one-step process.

Analytic solutions and numerical procedures have been attempted on the problem previously. Ingenito and Cook [3] have given an exact formulation for piston-like motions of the transducers with on-axis values given in approximation for a circular, rectangular, and square piston on its diagonal. Maloney, Meltz, and Gravel [4] have treated the square transducer with the Fresnel approximation. Their experimental measurements in solids agreed with theory for both axial and transverse profiles. Crandal [5] also made computations and measurements with emphasis on phase measurements for sound velocity measurements. Haran, Cook, and Stewart [6] have used the theoretical results for comparing optical calibration of a circular transducer with a radiation pressure technique. Riebold *et al.* [7], [8] have also made careful mea-

surements on the axis values to compare with the theory of Igenito and Cook [3]. Berlinghieri and Cook [9] have also calculated the  $v$ -field for a circular piston to test an inversion algorithm to estimate the pressure  $p(x, y, z)$  from measured values of  $v(x, z)$ .

The procedure presented here allows calculations throughout the near field including the adjacent region to the transducer where the pressure field and integrated optical effect can vary significantly with a small change of position. The only limitation in calculating the complete field appear to be those connected with the normal utilization of digital Fourier transforms.

THEORY

The procedure that is to be developed is based on the application of the Fourier projection slice theorem in conjunction with the Fourier technique of solving the scalar wave equations. Briefly the Fourier projection slice theorem states that the one-dimensional transform

$$W(k_x) = \int_{-\infty}^{\infty} w(x) \exp(ik_x x) dx \tag{2}$$

of the projection  $w(x)$ , defined as

$$w(x) = \int_{-\infty}^{\infty} f(x, y) dy \tag{3}$$

is equivalent to the two-dimensional Fourier transform  $F(k_x, k_y)$  with  $k_y = 0$ . In other words it states

$$W(k_x) = F(k_x, k_y = 0). \tag{4}$$

Consequently, a knowledge of a slice of Fourier domain yields  $w(x)$  upon the inverse transform. The theorem is to be applied to (1) which is now recognized as the form of a projection integral. Thus the scheme is to find the Fourier slice  $P(k_x, k_y = 0; z)$  corresponding to the local value  $p(x, y, z)$  of the pressure produced by a given normal particle velocity  $u(x, y, z = 0) e^{i\omega t}$  of the transducer; and then numerically compute the inverse transform.

A common method of approaching scalar radiation problems is by resolving the field parameter, i.e., pressure, velocity potential, etc., into a system of plane waves with two-dimensional Fourier transforms. For example, let

$$P(k_x, k_y; z) = \iint p(x, y, z) \exp[-i(k_x x + k_y y)] dx dy \tag{5}$$

and

$$p(x, y, z) = \left(\frac{1}{2}\pi\right)^2 \iint P(k_x, k_y; z) \cdot \exp[i(k_x x + k_y y)] dk_x dk_y \tag{6}$$

be a typical transform pair. Here  $p(x, y, z)$  is a phasor, as previously defined, that satisfies the Helmholtz equation

$$\nabla^2 p + k^2 p = 0 \tag{7}$$

as in the case of linear nonabsorbing acoustic waves. Substituting (6) into (7), one can obtain

$$\frac{d^2 P}{dz^2} + (k^2 - k_x^2 - k_y^2) P = 0. \tag{8}$$

A solution of (8) is

$$P(k_x, k_y; z) = P(k_x, k_y; z_0) \exp[-ik_z(z - z_0)] \tag{9}$$

where  $k_z = (k^2 - k_x^2 - k_y^2)^{1/2}$ . Thus, this approach permits calculation of the field in the plane  $z$  from a knowledge of the field in the plane  $z_0$ . The quantity  $P(k_x, k_y; z)$  can be interpreted as the phasor description of plane waves with wave vector  $(k_x, k_y, k_z)$ . It is noted that  $k_z$  can be real, which means that the wave propagates, or imaginary which infers an evanescent wave.

Our intermediate objective is to find  $P(k_x, k_y; z)$  from the velocity distribution of the transducer. We started with one component of the force equation

$$\frac{\partial p}{\partial z} = -\rho \frac{\partial u_z}{\partial t} \tag{10a}$$

$$= -i\omega u_z \quad (\text{for harmonic waves}) \tag{10b}$$

where the  $z$  axis is in the direction normal to the transducer surface and  $\rho$  is the density of the medium. Substituting (9) for the pressure and a similar expression for the particle velocity into (10) one can find

$$P(k_x, k_y; z) = (k/k_z) \rho c U_z(k_x, k_y; z) \tag{11}$$

where  $c$  is the velocity of sound. Equation (11) is the plane wave relationship between pressure and particle velocity; the term  $(k/k_z)$  in the secant of the angle between the direction of propagation of the plane and the  $z$  direction when  $k_z$  is real.

At this stage of the development, we know how to evaluate  $v(x, z)$  from  $P(k_x, 0; z)$  and to calculate  $P(k_x, 0; z)$  at any plane  $z$  from  $P(k_x, 0; z_0)$  which are related to a Fourier domain description of the  $z$  component of the particle velocity  $u_z(k_x, 0; z_0)$ . To obtain  $u_z(k_x, 0; z_0)$  from the given particle velocity  $u_z(x, y, z_0)$ , we again apply the Fourier projection slice theorem. We take the projection of  $u_z(x, y, z_0)$  to be

$$\bar{U}_z(x, z_0) = \int u_z(x, y, z_0) dy \tag{12}$$

where the  $y$  direction is chosen to be the direction of light propagation. The one-dimensional transform of  $\bar{U}_z(x, z_0)$  is  $U_z(k_x, 0; z_0)$  our desired result.

Thus the procedure for calculating the field  $v(x, z)$  is as follows.

- 1) For a given direction of light propagation with respect to transducer geometry, calculate the projection of velocity by (12).
- 2) Numerically compute the one-dimensional Fourier transform to find  $U_z(k_x, 0; z_0)$ .
- 3) Divide by  $k_z$  and the other appropriate constants to obtain  $P(k_x, 0; z_0)$  as specified by (11).
- 4) Calculate  $P(k_x, 0; z)$  at desired plane  $z$  using (9).

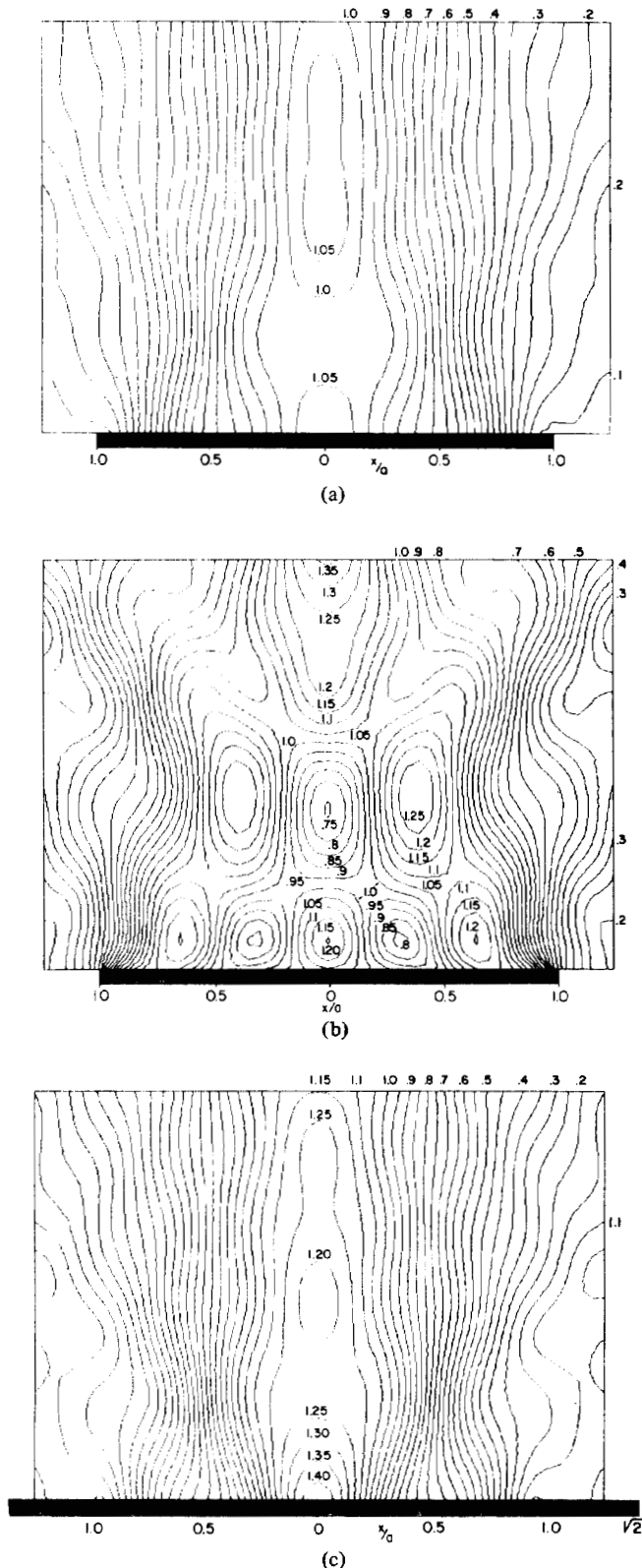


Fig. 3. Computed integrated optical effect (normalized for  $ka = 10$ ). (a) Circular transducer. (b) Rectangular. (c) Square on diagonal.

- 5) Compute the inverse one-dimensional transform to evaluate  $v(x, z)$ .

To calculate at alternate distance  $z$  from the transducer, repeat steps 4) and 5).

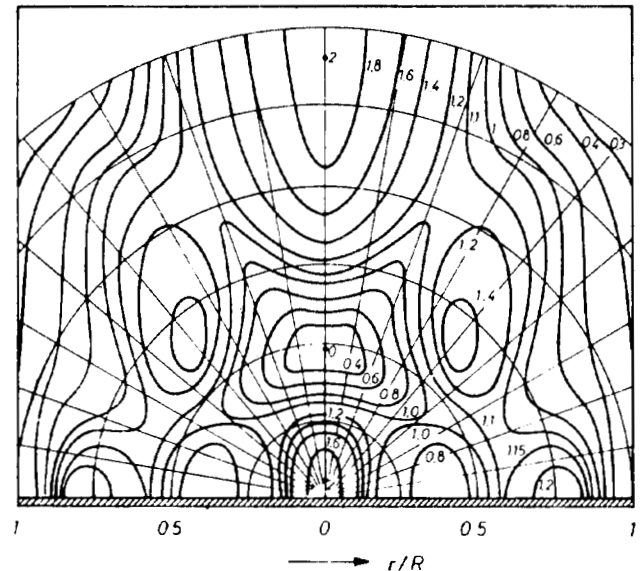


Fig. 4. Computed local variation of pressure for a circular piston with  $ka = 10$ , from Meyer and Newman [11]. (Courtesy of Academic Press).

## RESULTS

Using the procedure described above we have calculated the integrated optical effect for a circular, rectangular, and square transducer on its diagonal with  $ka = 10$ . The dimension  $a$  is the radius of a circular transducer, half the length of a side of the square transducer and half the length of the rectangular transducer perpendicular to the direction of light propagation. The field variations of  $v(x, z)$  for these configurations are shown in Fig. 3. Assuming the rectangular transducer is square the normalization  $v_0 = 4\pi ka/\lambda$  has been applied for all of these configurations.

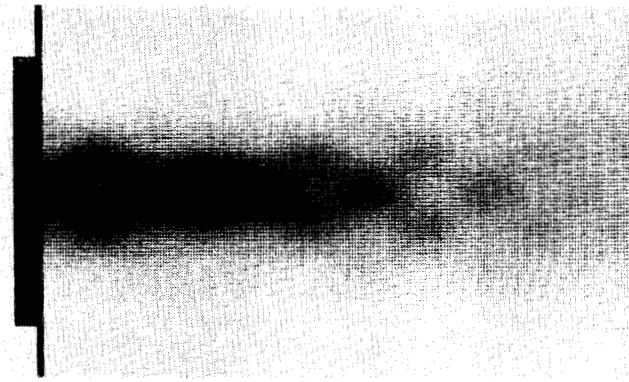
The field variations are observed to be considerably different in three configurations. The rectangular transducer has the largest variations, the circular next and the square on the diagonal being the most uniform. The results agree with the observations by Cook and Ingenito [10] and the calculations along the axis of Ingenito and Cook [3].

The variation in the integrated optical effect are not as large as the variations in the local value of pressure. Fig. 4 shows the variation in pressure generated by a circular transducer of  $ka = 10$  for comparison with Fig. 3(a).

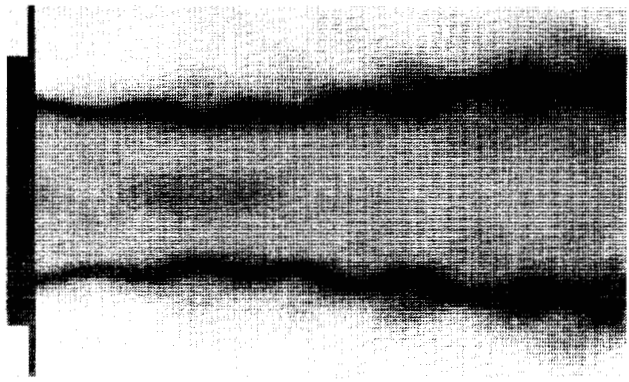
Having the field values of  $v(x, z)$  allows one to calculate photographs of schlieren patterns from first principles. To demonstrate how the transducer geometry and sound level affects the schlieren, we present a series of computed schlieren patterns. The spatial filter of the schlieren was chosen to pass only the zeroth diffraction order. The patterns were calculated by assigning each point in relative intensity

$$I_0 = J_0^2(v(x, z)) \quad (13)$$

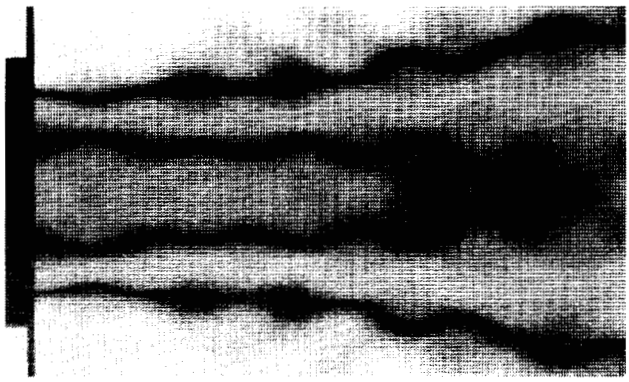
where  $J_0(v)$  is the zeroth order Bessel function of the first kind. A logarithmic response of the film was assumed and a gray scale assigned. Figs. 5, 6, and 7 correspond to the fields of Fig. 3(a), 3(b), and 3(c) at various sound levels. In each case the value of  $v$  listed is the maximum value found anywhere in the field. At low levels, there is a correspondence be-



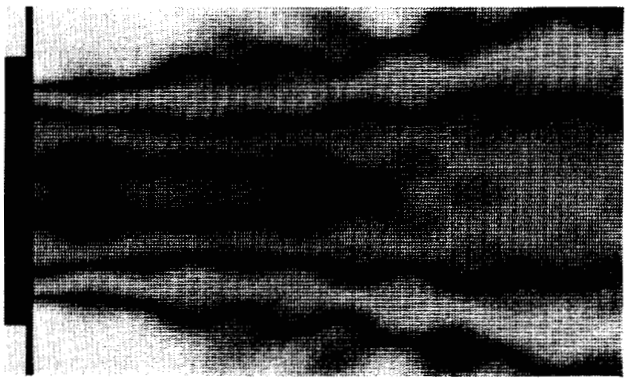
(a)



(b)

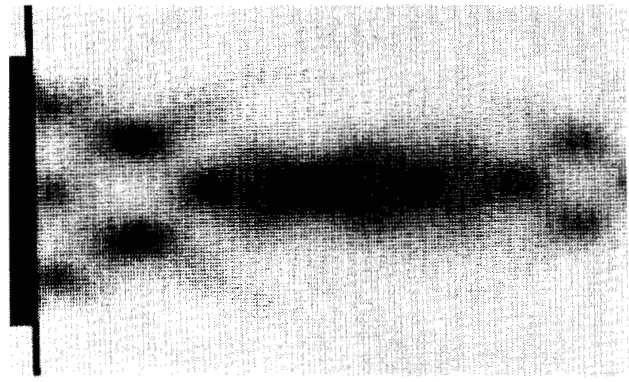


(c)

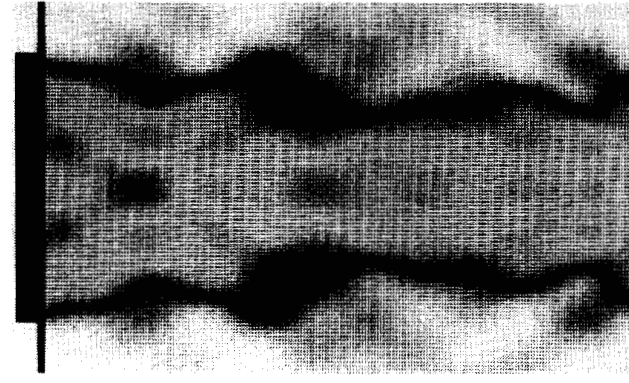


(d)

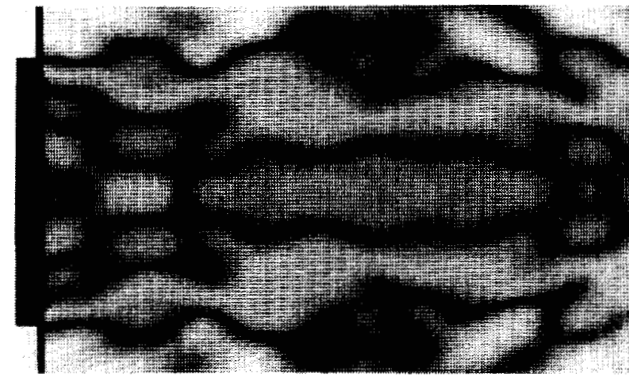
Fig. 5. Computed bright field schlieren for circular transducer at various sound levels. (a)  $\nu = 2.5$ . (b)  $\nu = 5.0$ . (c)  $\nu = 7.5$ . (d)  $\nu = 10.0$ .



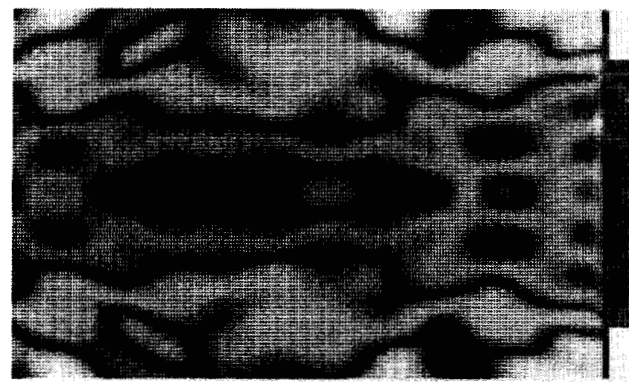
(a)



(b)



(c)



(d)

Fig. 6. Computed bright field schlieren for rectangular transducer at various sound levels. (a)  $\nu = 2.5$ . (b)  $\nu = 5.0$ . (c)  $\nu = 7.5$ . (d)  $\nu = 10.0$ .

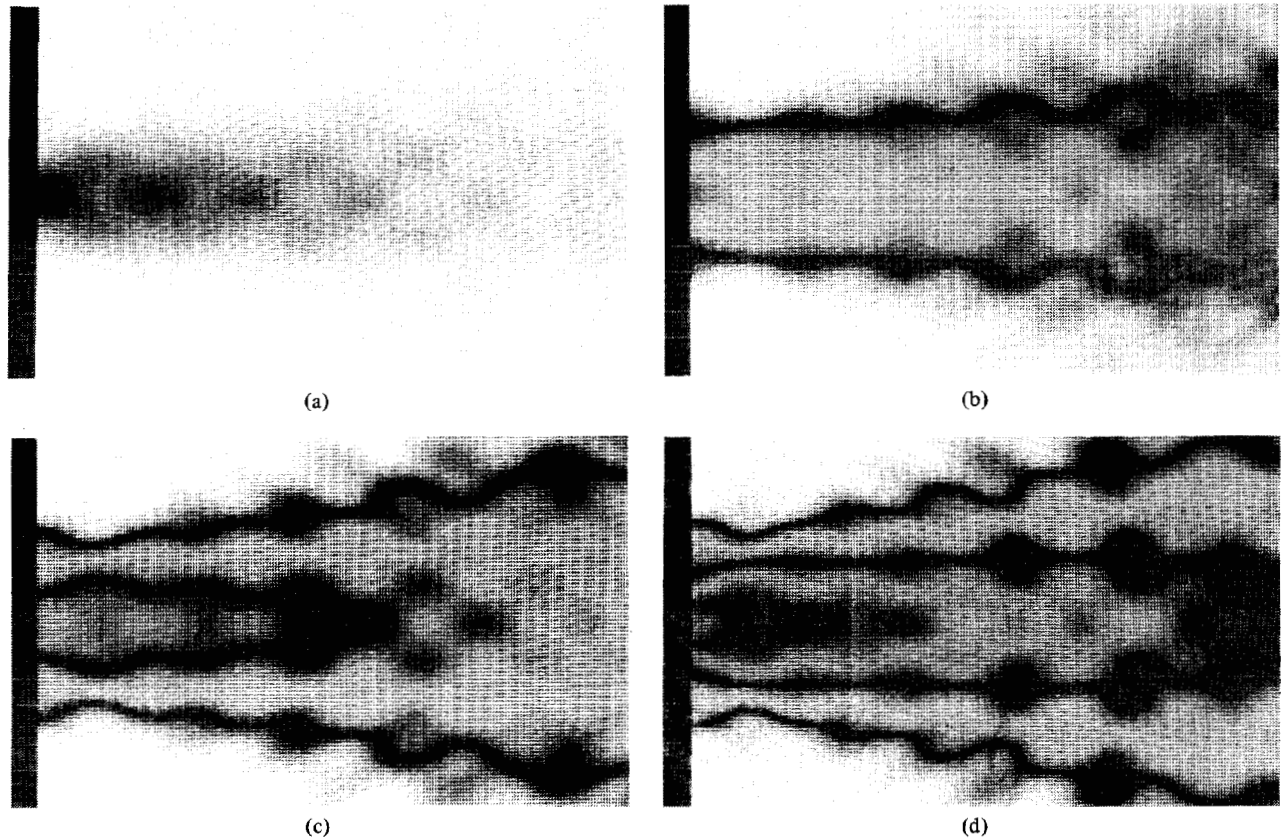


Fig. 7. Computed bright field schlieren for square transducer on its diagonal. (a)  $\nu = 2.5$ . (b)  $\nu = 5.0$ . (c)  $\nu = 7.5$ . (d)  $\nu = 10.0$ .

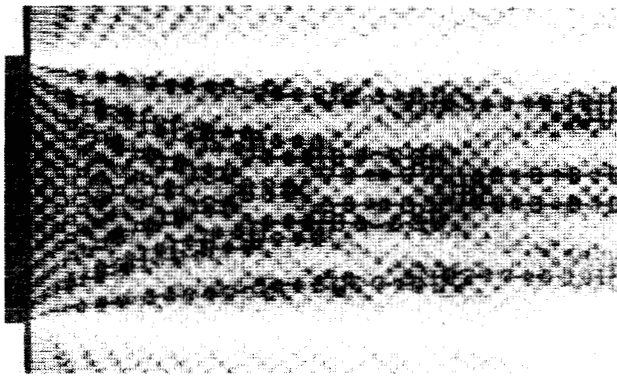


Fig. 8. Computed dark field schlieren approximating the conditions of Fig. 1 of a square transducer with  $ka = 45.2$ .

tween the gray levels and the field value of  $\nu$  in Fig. 3. However, at higher sound levels, the nonlinear properties of (13) tends to make the patterns more complicated and less interpretable. However, the spreading nature of the sound beam becomes more evident at the higher levels.

An increase of  $ka$  also changes the pattern. From the description of Osterhammel's experimental arrangement and an estimation of the sound level, we have computed the image shown in Fig. 8 which is to be compared with Fig. 1. As one can see, many of the geometrical features are duplicated in the calculated image. In fact, the computed image contains some gray areas which are in the original photographs but have been lost in subsequent photographic reproductions. For the pat-

tern shown in Fig. 8, we have chosen a spatial filter that passes only the first diffraction orders. Consequently, intensity assigned to each point is the square of the first-order Bessel function with the argument  $\nu$ . Other schlieren patterns are shown elsewhere [11].

#### CONCLUSION

From first principles it is possible to calculate the integrated optical effect for any given transducer configuration in the Raman-Nath region. The numerical technique results from application for Fourier projection slice theorem and does not require explicit integration. Implementation via FFT permits rapid calculations of the integrated optical effect and schlieren patterns.

This procedure can be adapted easily to other configurations such as focused transducers, imperfect transducers, zone plates, and shaded transducers.

#### ACKNOWLEDGMENT

The authors wish to thank Dr. George Batten, University of Houston, for his assistance with the computer graphic techniques.

#### REFERENCES

- [1] K. Osterhammel, "Optische Untersuchung des Schallfeldes Kolbenförmig Schwinger Quarze," *Akust. Z. Bd. 6*, pp. 73-86, 1941.
- [2] W. R. Klein and B. D. Cook, "Unified approach to ultrasonic

- light diffraction," *IEEE Trans. Sonics Ultrason.*, vol. SU-14, pp. 123-134, 1967.
- [3] F. Ingenito and B. D. Cook, "Theoretical investigation of the integrated optical effect produced by sound fields radiated from plane piston transducer," *J. Acoust. Soc. Am.*, vol. 45, pp. 572-577, 1969.
- [4] W. T. Maloney, G. Meltz, and R. L. Gravel, "Optical probing of the Frensel and Fraunhofer regions of a rectangular acoustic transducer," *IEEE Trans. Sonics Ultrason.*, vol. SU-15, pp. 167-172, 1968.
- [5] A. J. Crandal, "Measurement of the velocity of sound in water by optical methods," Ph.D. thesis, Department of Physics, Michigan State University, East Lansing, University Microfilms No. 68-7882.
- [6] M. E. Haran, B. D. Cook, and H. F. Stewart, "Comparison of an acoustooptic and a radiation force method of measuring ultrasonic power," *J. Acoust. Soc. Am.*, vol. 57, pp. 1436-1440, 1975.
- [7] R. Riebold, W. Molkenstruck, and K. M. Swamy, "Experimental study of the integrated optical effect of ultrasonic fields," *Acustica*, vol. 43, pp. 253-259, 1979.
- [8] R. Riebold, "The measurement of ultrasonic power using an acousto-optic method," *Acustica*, vol. 36, pp. 214-220, 1976/1977.
- [9] J. C. Berlinghieri and B. D. Cook, "Data requirements for mapping of ultrasonic fields with conventional light diffraction," *J. Acoust. Soc. Am.*, vol. 58, pp. 823-827, 1975.
- [10] B. D. Cook and F. Ingenito, "Ultrasonic transducer configuration for producing a phase grating of nearly uniform strength," *Proc. IEEE*, vol. 56, pp. 871-872, 1968.
- [11] B. D. Cook, "A procedure for calculating the integrated acoustooptic (Raman-Nath) parameter for the entire sound field," presented at the 1979 Ultrasonic Symp., New Orleans, LA, Sept. 26-28, 1979, paper p-8.
- [12] E. Meyer and E. Newman, *Physical and Applied Acoustics: An Introduction*. New York and London: Academic, 1972, p. 175.
-